Manganese-doped ZnO nanobelts for spintronics

C. Ronning,[a] P. X. Gao, Y. Ding, and Z. L. Wang[b]
School of Materials Science, Georgia Institute of Technology, 771 Ferst Drive, Atlanta, Georgia 30332-0245

D. Schwen
II. Physikalisches Institut, Universität Göttingen, Tammannstr. 1, 37077 Göttingen, Germany

Zinc oxide (ZnO) nanobelts synthesized by thermal evaporation have been ion implanted with 30 keV Mn^+ ions. Both transmission electron microscopy and photoluminescence investigations show highly defective material directly after the implantation process. Upon annealing to 800 °C, the implanted Mn remains in the ZnO nanobelts and the matrix recovers both in structure and luminescence. The produced high-quality ZnO:Mn nanobelts are potentially useful for spintronics. © *2004 American Institute of Physics.* [DOI: 10.1063/1.1645319]

Diluted magnetic semiconductors (DMS) are one of the promising materials for spintronics (spin+electronics), a proposed technology that uses the electron spin rather than the electron charge for reading and writing informations.[1,2] Much of the recent effort toward spintronics has been focused on the synthesis and characterization of manganese doped III-V and II-VI materials, with prominent interest in GaN:Mn and ZnO:Mn due to a proposed and measured Curie temperature above room temperature.[3,4]

The integration of DMS materials into today's electronics will require very low dimensions in order to make real use of the advantage offered by the spin, but the majority of the recent studies are focused on bulk materials. Furthermore for the future goal, a doping technique of nanosized structures has to be established, offering precise control of the species in both concentration and lateral position. In this article, we report on the successful combination of ion implantation and semiconducting nanobelts[5] in order to realize a nanosized quasi-one-dimensional DMS for the possible use in spintronics.

Single crystalline ZnO nanobelts have been synthesized by thermal evaporation of ZnO powder at a temperature of 1350 °C in a tube furnace under 50 sccm argon gas flow at a pressure of 300 mbar for 1 h.[5] The as-deposited nanobelts onto silicon (100) substrates at the colder end of the tube have a ribbon shape with uniform geometry and dislocation-free volume; they are up to 100 μm long, between 40–500 nm wide, and between 10–40 nm thick, as determined by scanning electron microscopy (SEM) and investigated in detail elsewhere.[5] Electron dispersive spectrometry (EDS) revealed the only presence of stoichiometric zinc and oxygen signals. Ion implantation of $^{55}Mn^+$ ions into the ZnO nanobelts were carried out at room temperature with an ion energy of 30 keV and a fluence of 1×10^{15} cm^{-2}. The corresponding ion range is 16 nm with a straggling of 7 nm, and the corresponding Mn peak concentration is about 1 at. %, as calculated with the program package TRIM.[6] Conventional and high resolution transmission electron microscopy (TEM)

images were obtained using both Hitachi HF-2000 FEG (equipped with EDS) and JEOL 4000EX electron microscopes operating at an accelerating voltage of 200 and 400 keV, respectively. Annealing of the Mn-implanted ZnO-nanobelts was performed for 10–15 min at 800 °C under high vacuum conditions ($\sim 10^{-5}$ mbar). Photoluminescence (PL) investigations were done using a He–Cd laser, a 1 m Cerny–Turner spectrograph, and a photomultiplier.

The overall morphology in size and length of the ZnO nanobelts did not change upon the implantation process, as observed by SEM. On the other hand, the density and structure of the defects introduced into the nanobelts has been investigated in detail using high resolution TEM, as summarized in Fig. 1. The representative 65 nm wide ZnO nanobelt shown in Fig. 1(a) directly after ion-implantation had a growth direction along the $[01\bar{1}0]$ axis, which is evident by the diffraction pattern shown in Fig. 1(b). A continuous nanosize stacking fault throughout the nanobelt is visible in the middle region and is common for this type of ZnO nanobelts due to the synthesis process.[5] The implanted nanobelt shows a rough edge in contrast to non-implanted nanobelts, which is due to the sputtering of individual surface atoms during implantation. Furthermore, it is obvious that the implantation process created no amorphous areas even with such a high implantation fluence. However, a high density of extended implantation defects (stacking faults) is clearly visible within the complete nanobelt by the contrast change between dark and bright spots. An estimation of the density results to about 2.5($\pm$0.5) extended defects per 100 nm^2, which is about 400 times less compared to the implantation fluence. A detailed back and forth fast Fourier transformation (FFT) analysis using only the $\pm$(0002) diffraction spots of one representative stacking fault is displayed in Fig. 1(e), showing that a pair of edge dislocations is created very close to each other within the (0001) planes. This is due to the presence of a dislocation loop created by the ion implantation process. The appearance of an opposite dislocation pair is very reasonable, because no additional planes can be introduced to the overall lattice with an implantation process. In addition to the planar defects, the areas in-between indicate the presence of point defects like interstitials and vacancies. Figure 1(c) is a high-resolution TEM image cutout of

---
[a]On leave from: II. Physikalisches Institut, Universität Göttingen; electronic mail: carsten.ronning@phys.uni-goettingen.de
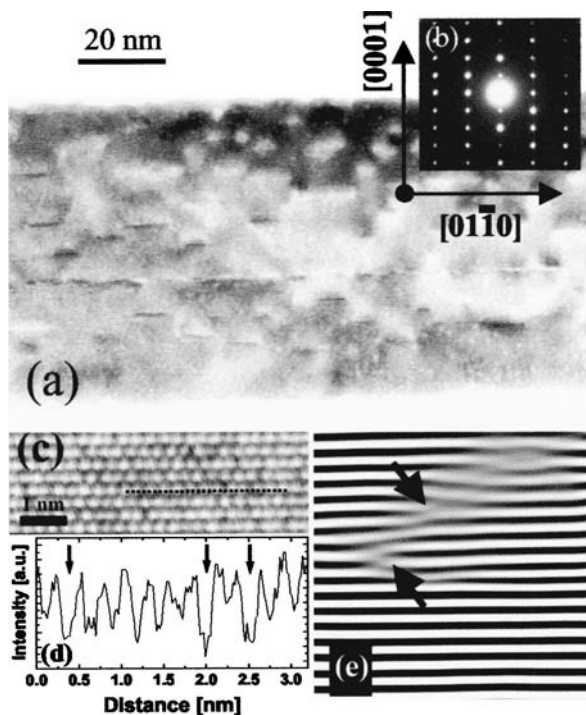[b]Electronic mail: zhong.wang@mse.gatech.edu

FIG. 1. As-implanted situation of a Mn-implanted ZnO nanobelt. (a) TEM micrograph showing a high defect density and (b) corresponding diffraction pattern. The chart (c) shows a high-resolution cutout of (a) and (d) is an intensity scan along the dotted line within (c). (d) The back and forth fast Fourier transformation (FFT) analysis using the 000 ± 1 diffraction spots of an extended defect shows a pair of dislocations next to each other within the (0001) planes.

Fig. 1(a) that shows irregular dark and bright points; and a line scan along an arbitrary chosen (0002) plane that is displayed in Fig. 1(d) demonstrates also an irregular oscillation. This analysis was done for several areas and planes and always revealed a high density of dark points as indicated by the three arrows in Fig. 1(d), which might be due to one or more additional interstitial atoms along the TEM beam direction of $[2\bar{1}\bar{1}0]$.

The collision cascade of one single implanted Mn ion creates about 300 vacancies and respective interstitials in bulk ZnO.[6] If we compare this number with our defect densities observed above, we can conclude that the majority of the created defects recombine already by dynamic annealing within the thermal spike following the collision cascade resulting in a very resistant material against irradiation, which is in agreement with Refs. 7 and 8. Such a high dynamic annealing behavior of the ZnO nanobelts is reasonable, because of two factors: (a) the ZnO material itself has a high bonding ionicity, which forces displaced atoms back into their respective places in the periodic charged lattice by coulomb interaction; and (b) due to the small size of the nanobelts a further enhancement of the dynamic annealing can be expected by the comparable longer duration for the dissipation of the introduced implantation energy in the confined geometry.[9]

Figure 2 shows EDS spectra (taken in TEM) for one ZnO nanobelt directly after Mn ion implantation (top) and after annealing to 800 °C for 15 min under high vacuum conditions (bottom), which was performed *in situ* in the TEM. The Si, C, and Cu signals are originating from the TEM grid, but visible are also the stoichiometric Zn and O
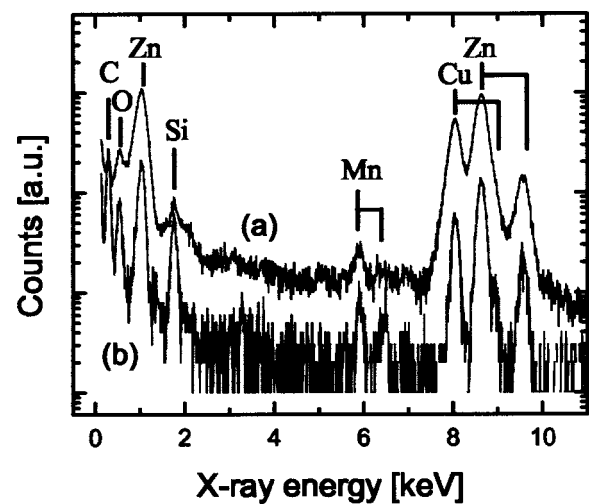

FIG. 2. Energy dispersive spectrometry (EDS) spectra of Mn-implanted ZnO-nanobelts (a) directly after ion implantation and (b) after subsequent annealing to 800 °C.

signals of the nanobelt as well as the signal of the implanted Mn atoms. The Mn peak intensity is consistent with the desired doping concentration of about 1 at. %. The annealing procedure definitely does not result into an out-diffusion of the implanted Mn, which is not in agreement with Ref. 7 observing the onset of Mn-diffusion in ZnO already at 700 °C. The difference is most probably due to the confined geometry as well as the different quality of the ZnO material.

The structure and density of the defects after the annealing procedure investigated with TEM are summarized for comparison in Fig. 3 in the same manner as in Fig. 1. A representative about 500 nm wide ZnO nanobelt with the same growth direction as the nanobelt show in Fig. 1 reveals a much lower density of defects, as is clearly visible in Fig. 3(a). An estimation of the average density gives $0.2(\pm0.1)$ extended defects per 100 nm^2, about one order of magnitude lower than that of the as-implanted sample. On the other hand, it is evident that the dimension of the extended defects increased. The corresponding back and forth fast Fourier transformation (FFT) analysis of one representative extended defect demonstrate that the pair of edge dislocations are more apart from each other compared to Fig. 1(e), e.g., 11 planes for the case shown in Fig. 3(d). However, the areas in-between the extended defects are almost perfectly periodic, indicating the removal of the majority of the point defects like vacancies and interstitials. This is evident in both the high-resolution cutout shown in Fig. 3(b) as well as in the respective line scan in Fig. 3(c) showing the regular intensity oscillations of the (0001) planes.

On this basis, we conclude that the majority of the created implantation defects are removed upon the annealing procedure to 800 °C by diffusion of both vacancies and interstitials, in agreement with Refs. 10 and 11. However, some vacancies and interstitials are trapped by the only few remaining edge dislocations or loops resulting into an increased size of the extended defect. Higher annealing temperatures are necessary in order to remove such a type of extended defects; however, a diffusion of the implanted Mn also may occur out of the lattice above 800 °C.[10] Our observed results are consistent with studies claiming the com-
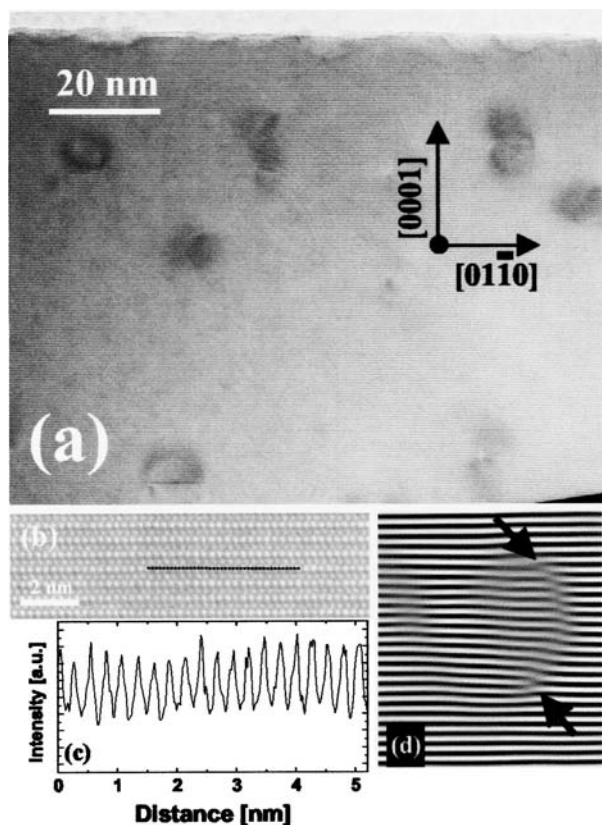
FIG. 3. A Mn-implanted ZnO nanobelt after annealing to 800 °C. (a) TEM micrograph showing a reduced defect density. The chart (b) shows a high-resolution cutout of (a) and (c) is an intensity scan along the dotted line within (b) demonstrating a more regular oscillation compared to Fig. 1(d). (d) The back and forth FFT analysis using the 000 ± 1 diffraction spots of an extended defect shows a widely apart pair of dislocations within the (0001) planes.

FIG. 4. Photoluminescence spectra of ZnO nanobelts with and without Mn implantation recorded at 12 K after annealing at 800 °C for 10 min.

plete removal of all implantation defects in ZnO and the activation of the implanted species after annealing,[7,10,12] because the applied techniques in that investigations are not that sensitive on the observation of defects like TEM used in this study. Anyway, the optical, magnetic, and electrical activation of the implanted species does not require a complete removal of all defects, but a recovery of the majority of the crystal lattice as well as the implementation of the implanted species into the desired lattice sites.

These statements are supported by our PL studies performed on the Mn implanted nanobelts. In our case, the luminescence intensity of the Mn doped nanobelts was suppressed by several orders of magnitude directly after the ion implantation process. However, as shown in Fig. 4, it is obvious that the luminescence has been completely recovered after the annealing step at 800 °C for 10 min and reaches the intensity of the unimplanted control sample. For both samples, the sharp ultraviolet (UV) emission of the band edge luminescence is clearly visible at $3.36(\pm 1)$ eV as well as the corresponding first phonon replica at $3.31(\pm 1)$ eV, resulting in a longitudinal optical phonon energy around 60 meV in agreement with Ref. 13. An additional signal from the implanted Mn ions has been not expected, because Mn does not form any acceptor or donor levels within ZnO. However, a slight difference of the luminescence of the implanted and control sample can be observed for the very
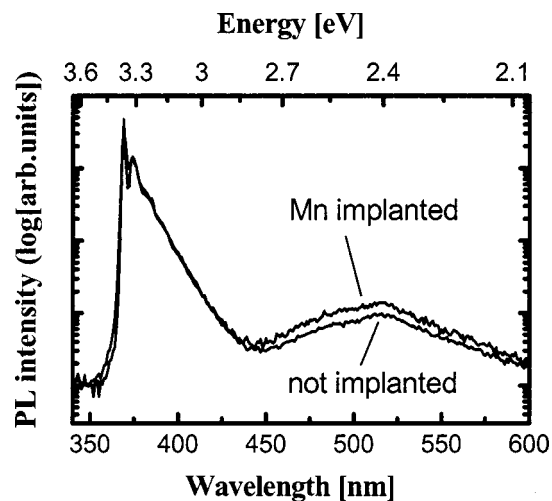
weak board green band centered at 510 nm (please, note the logarithmic scale of Fig. 4). This luminescence band of deep levels within the band gap originates from defects and has been assigned to oxygen vacancies[14] or incorporated Cu^{2+} ions[15] and is usually orders of magnitude more intense in bulk thin films.[12,13] We conclude from our experiment that this green emission results from point defects created upon implantation (e.g., vacancies or interstitials) and can be annealed out to a large extent.

In view of both the TEM and PL results, the quality of the resulting Mn doped ZnO nanowires is fairly high compared to bulk ZnO films[12,13] and ZnO nanorods.[16]

[1] G. A. Prinz, Science **282**, 1660 (1998).
[2] J. K. Furdyna, J. Appl. Phys. **64**, R29 (1988).
[3] T. Dietl, H. Ohno, F. Matsukura, J. Cibert, and D. Ferrand, Science **287**, 1019 (2000).
[4] K. Ueda, H. Tabata, and T. Kawai, Appl. Phys. Lett. **79**, 988 (2001).
[5] Z. W. Pan, Z. R. Dai, and Z. L. Wang, Science **291**, 1947 (2001).
[6] J. F. Ziegler, J. P. Biersack, and U. Littmark, The *Stopping and Ranges of Ions in Solids* (Pergamon, New York, 1985). See also www.srim.org.
[7] E. Sonder, R. A. Zuhr, and R. E. Valiga, J. Appl. Phys. **64**, 1140 (1988).
[8] S. O. Kucheyev, J. S. Williams, C. Jagadish, C. Evans, A. J. Nelson, and A. V. Hamza, Phys. Rev. B **67**, 094 115 (2003).
[9] S. Dhara, A. Datta, C. T. Wu, Z. H. Lan, K. H. Chen, Y. L. Wang, L. C. Chen, C. W. Hsu, H. M. Lin, and C. C. Chen, Appl. Phys. Lett. **82**, 451 (2003).
[10] D. P. Norton, S. J. Pearton, A. F. Hebard, N. Theodoropoulou, L. A. Boatner, and R. G. Wilson, Appl. Phys. Lett. **82**, 239 (2003).
[11] S. O. Kucheyev, C. Jagadish, J. S. Williams, P. N. K. Deenapanray, M. Yano, K. Koike, S. Sasa, M. Inoue, and K. Ogata, J. Appl. Phys. **93**, 2972 (2003).
[12] T. Monteiro, C. Boemare, M. J. Soares, E. Rita, and E. Alves, J. Appl. Phys. **93**, 8995 (2003).
[13] D. Kim, T. Terashita, I. Tanaka, and M. Nakayama, Jpn. J. Appl. Phys., Part 2 **42**, L935 (2003).
[14] K. Vanheusden, W. L. Warren, C. H. Seager, D. R. Tallant, J. A. Voigt, and B. E. Gnade, J. Appl. Phys. **79**, 7983 (1996).
[15] N. Y. Garces, L. Wang, L. Bai, N. C. Giles, L. E. Halliburton, and G. Cantwell, Appl. Phys. Lett. **81**, 622 (2002).
[16] S. C. Lyu, Y. Zhang, H. Ruh, H. J. Lee, H. W. Shim, E. K. Suh, and C. J. Lee, Chem. Phys. Lett. **363**, 134 (2002).